On the re-initiation of an attenuated detonation wave following an abrupt area expansion

Mohnish Peswani[1] and Brian Maxwell[1,2]
[1]Department of Mechanical and Aerospace Engineering, Case Western Reserve University
Cleveland, Ohio, USA
[2]Department of Mechanical Engineering, University of Ottawa, Ontario, Canada

1 Introduction

When a detonation undergoes diffraction, the detonation can be extinguished (sub-critical outcome) or successfully propagated (super-critical outcome), depending on the tube diameter. There also exists a critical tube diameter (D_c), which separates the sub-critical and super-critical outcomes where the detonation wave is re-initiated by a transverse detonation wave that propagates in the shocked and unreacted mixture created as a result of the sudden area expansion. Despite several decades of research, however, a predictive model for the critical outcome following detonation diffraction in hydrocarbon mixtures is still lacking. This is, in part, due to the vast majority of numerical studies adopting simple one- or two-step combustion models that do not adequately resolve the cellular instabilities in hydrocarbon mixtures that exhibit a characteristically irregular detonation structure. To address this deficiency, we recently revisited the detonation diffraction problem numerically in ethylene–oxygen mixtures [1] using a thermochemically derived four-step combustion model [2]. By providing the necessary chemical accuracy, the numerical simulations successfully captured the different regimes following diffraction successfully observed experimentally. Moreover, the re-initiation of the attenuated detonation by the transverse detonation was successfully observed in the critical regime, and D_c was found to agree with the well-known 13λ correlation.

In the aforementioned numerical study, detonation quenching and re-initiation were observed for initial pressures of $p_0 = 13.75$ kPa and 13.8 kPa. Figure.1 summarizes the results from the simulation conducted with $p_0 = 13.8$ kPa. For this critical pressure, a transverse detonation that propagated to the back wall in the shocked but unreacted gas mixture shown in Fig.1a was found to be triggered as a result of explosions caused by triple-point collisions in the vicinity of unburned gas pockets along the diffracting detonation. While the transverse detonation temporarily re-coupled the shock front and reaction zone, it failed the re-initiate the detonation in the full channel. Instead, following the reflection of this re-coupled front with the top boundary shown in Fig.1b, the detonation in the channel was fully re-established via a detonation triggered along the Mach shock at the top boundary as well as via a second transverse detonation that propagates in the shocked–unreacted gas mixture along the detonation front from the top boundary to the tube axis. The re-initiation along the Mach shock and the second transverse detonation are shown in Fig.1c. Another observation from the numerical study was that the triple point attached to the second transverse detonation was overdriven relative to the quiescent mixture. The triple points under consideration here are the locations where the incident shock, decoupled detonation front, and transverse detonation meet and are shown as TP1 and TP2 in Figs. 1a and 1c. In the current study, we investigate in more detail the mechanisms by which the detonation is re-initiated in the channel following the boundary reflection and provide an explanation for the overdriven triple point.

Correspondence to: mohnish.peswani@case.edu

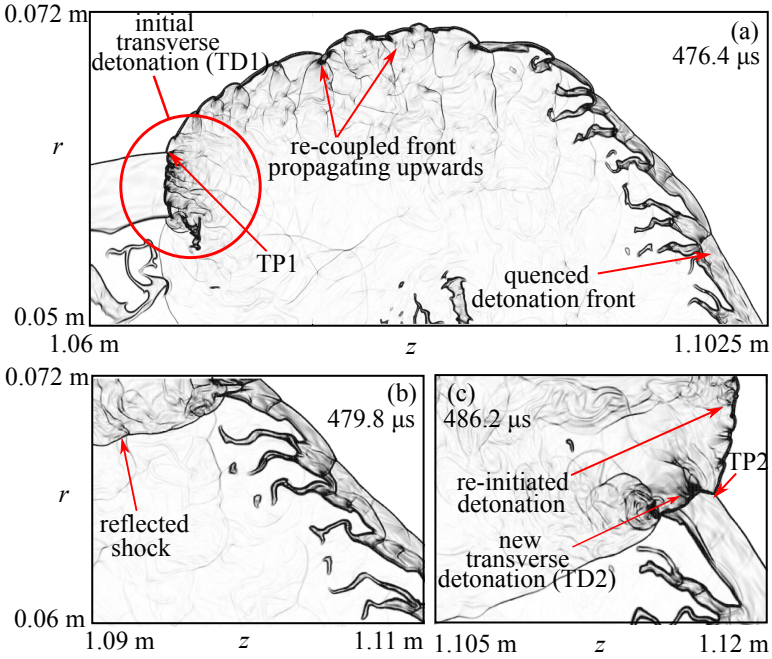

Figure 1: Density gradient evolution showing the first transverse detonation (a) and subsequent detonation re-initiation in the channel (b and c) for $p_0 = 13.8$ kPa.

2 Numerical Approach

The numerical domain selected was identical to the experimental setup of Schultz [3], with a detonation initially propagating in an axi-symmetric tube with an internal diameter of 36 mm before undergoing a 90°expansion into a 144 mm wide channel, as shown in Fig. 2. To trigger the detonation wave, an initially overdriven Zel'dovich-von Neumann-Doring (ZND) solution was imposed at $z = 0$ that was oriented to propagate to the right in the positive $z-$direction. The right boundary condition is a zero-gradient type, while the remaining boundaries are symmetric types in which only the normal velocity components are reversed. The tube length of 1.05 m was found to be sufficiently long to permit the overdriven detonation wave to settle to within 1% of the CJ-detonation speed by the time the wave reached the corner for all initial pressures and resolutions considered. For all simulations, the quiescent mixture composition was stoichiometric ethylene-oxygen ($C_2H_4 + 3O_2$), with an initial temperature $T_0 = 300$ K.

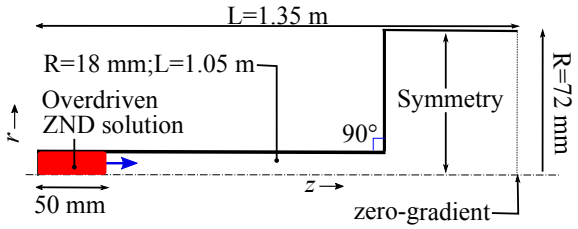

Figure 2: Numerical set-up, with a zero-gradient condition on the right boundary, and symmetric elsewhere.

To simulate the detonation diffraction out of a tube, the two-dimensional axi-symmetric reactive Euler equations were solved using a compressible flow solver with adaptive mesh refinement (AMR) capability. Since detailed hydrocarbon chemistry descriptions are not amenable to high-resolution simulations, we instead applied a thermochemically derived four-step global reaction mechanism [2] calibrated for

ethylene–oxygen combustion to provide the necessary chemical accuracy. Specific details about the species production rates in the model can be found elsewhere [2]. The base grid resolution for simulations conducted was 5 mm, with anywhere between 6 to 9 additional levels of refinement applied, depending on the desired minimum grid resolution. Results are presented for 9 AMR levels of refinement, which corresponds to a minimum resolution of 20 μm or ≈ 5 - 10 grid points per ZND induction length depending on the initial pressure of the quiescent mixture. For complete details about the governing equations solved, the AMR criteria, and the influence of grid resolution on the results, please refer to the manuscript by Peswani et al. [1]

3 Re-initiation mechanism for the second transverse detonation

To gain more clarity on the formation of the detonation waves observed in Fig.1c, detailed density gradient, temperature, and local ignition delay profiles are shown in Fig. 3 for time steps immediately following the reflection of the diffracted wave with the top boundary. In Fig.3, frame (a) at $t = 478.2$ μs shows the reflected shock wave (sw1) from the top boundary just prior to its interaction with the burned–unburned gas interface (f1). In frame (b) at $t = 478.8$ μs, the interaction of the shock wave and interface led to enhanced burning rates with a localized explosion accompanied by an increase in temperature observed. These enhanced burning rates were likely due to Richtmyer-Meshkov instabilities that arose from the passage of the reflected shock wave through the flame surface. Following the explosion, sw1 is then observed to propagate into the gas which contained favorable ignition delay times behind the Mach shock as shown in frame (c) at $t = 481.0$ μs. The detonation wave along the Mach shock (d1) shown in frame (d) then appears to be triggered directly by the local pressure amplification due to the explosion which led to a rapid coupling of the shock and reaction zones. For both pressure cases ($p_0 =$ 13.75 kPa and 13.8 kPa) where re-initiation was observed, the detonation along the Mach shock was established first. The transverse detonation (d2) is then found to be initiated directly by the passage of the reflected shock wave over multiple burned–unburned interfaces along the expanding detonation front. The established transverse detonation is shown in frame (e) at $t = 482.8$ μs.

Figure 4 shows the pressure and log(ignition delay) profiles measured at different times along the top boundary at $r = 0.072$ m in the frame of reference of the leading wave front. First, at $t = 482.8$ μs, a large pressure spike is observed at the location where the initial explosion is observed when the shock wave passes through the reaction front. According to the pressure profiles, sw1 then clearly experiences a pressure amplification through time due to the enhanced burning rates and by propagating against the ignition time gradient shown in the delay time profiles. The mechanism of detonation initiation thus resembles the well-known SWACER (Shock Wave Amplification by Coherent Energy Release) mechanism [4]. In this case, however, the initial explosion was driven and enhanced through Richtmyer-Meshkov instabilities by the passing of an external shock wave over an existing hot spot and not started by the spontaneous ignition of the gas having minimum ignition delay. Upon measuring the ignition delay time gradient ahead of the reaction wave, we found that the inverse of the ignition delay was $(\nabla\tau_{\mathrm{ig}})^{-1} \sim 2252$ m/s only right before the wave front, at all times. Ahead of the wave, $(\nabla\tau_{\mathrm{ig}})^{-1}$ was only $\mathcal{O}$(1 to 200) m/s. This observation is, in fact, consistent with the past work of Kuznetsov et al. [5] where the $(\nabla\tau_{\mathrm{ig}})^{-1}$ of the pre-heated mixture during DDT of ethylene–oxygen was also much less than the CJ-detonation speed. In fact, the recent work of Wang et al. [6] demonstrates that detailed mechanisms are able to permit detonation initiation in much shallower ignition delay gradients compared to simple combustion models (i.e. the one-step combustion model). Although we applied a fairly simple 4-step global combustion model, we have demonstrated its ability to at least mimic a wide spectrum of detailed ignition delay times, and steady detonation profiles [2]. Although gradients in τ_{ig} were shallow in this case, it is important to point out that non-uniformities did exist in the ignition delay time profiles

of Figs. 3 and 4, and that such gradients may have promoted the propagation of the reaction wave until a sustained detonation has formed.

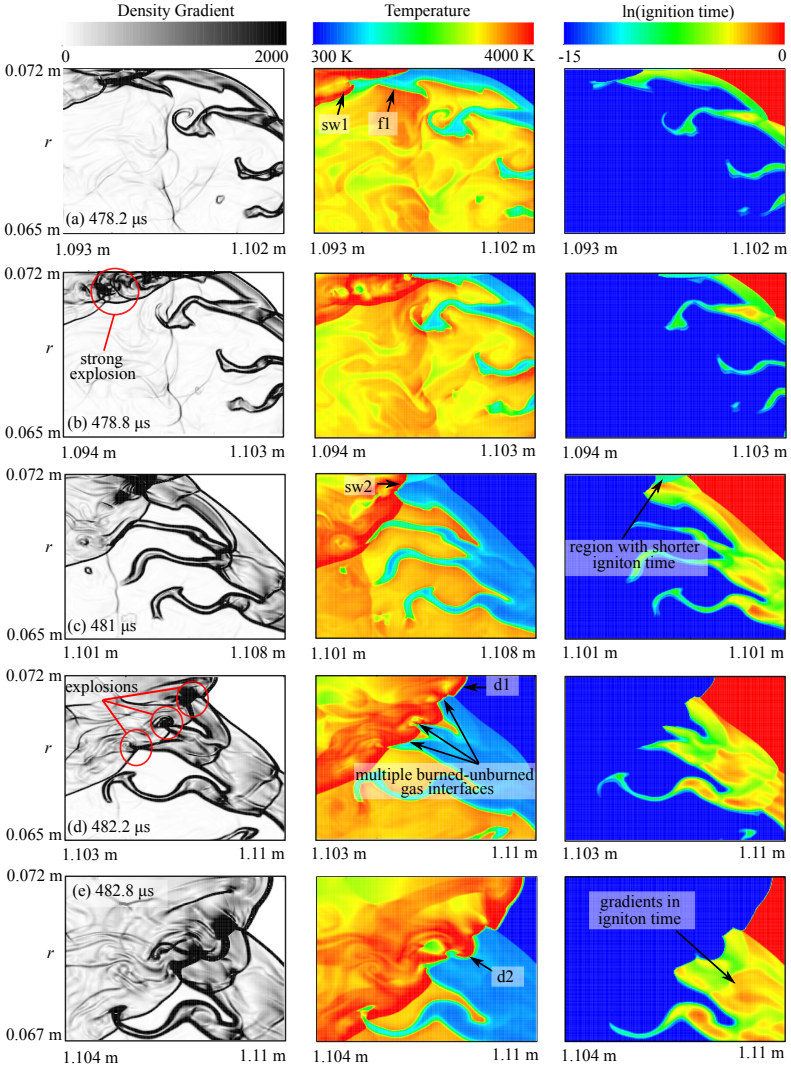

Figure 3: Details of the density gradient, temperature, and ignition delay times for detonation re-initiation with $p_0 = 13.8$ kPa.

4 The overdriven second triple point

In the study by Peswani et al. [1], the triple point and transverse detonation speeds were measured for cases where re-initiation of the attenuated detonation wave was observed. In general, it was found that both transverse detonations (TD1 and TD2) were CJ detonations relative to the shocked and unburned gas mixture through which they propagate. Moreover, while the triple point attached to the first transverse detonation (TP1) was found to propagate at the theoretical CJ speed of the quiescent mixture (within +5%), the triple point attached to the second transverse detonation (TP2) was overdriven by approximately 12%. Since the transverse detonation attached to TP2 is a CJ detonation, and the detonation established along the Mach shock following the reflection was found to be only briefly overdriven, a more detailed investigation is needed to understand the overdriven nature of TP2. To estimate the speed

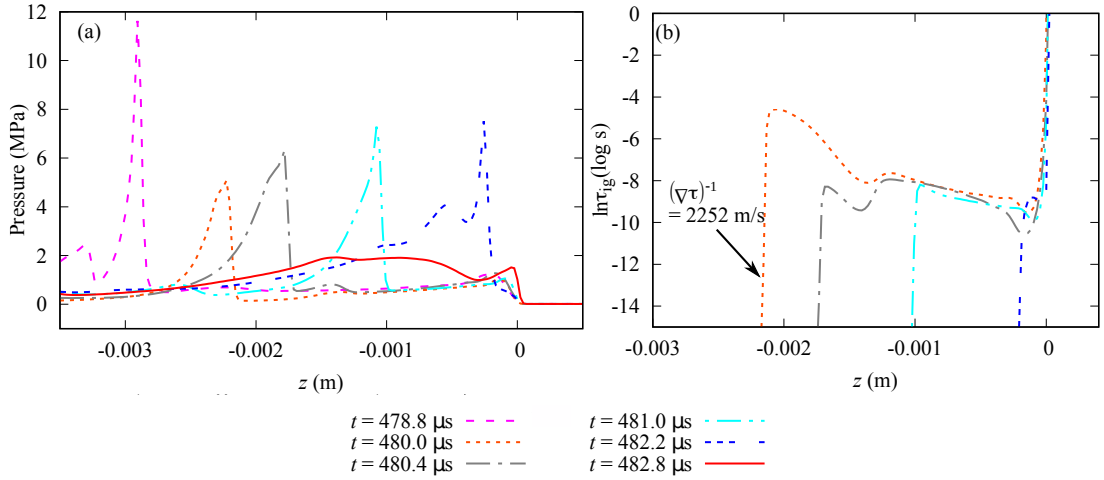

Figure 4: Pressure and ignition delay time profiles measured along $r = 0.072$ m for $p_0 = 13.8$ kPa.

of the transverse detonation, in the study, the velocity vector of the triple point speed relative to the velocity vector of the shocked gas in front of the transverse detonation was considered. The triple point was chosen as a reference point since its absolute lab frame velocity can be assumed to be close to that of the transverse detonation. To determine the velocity of the shocked gas in front of the transverse wave, a sample space with an approximate area of 12.25 mm^2 consisting of, on average, 25,000 points on the finest refinement level was considered. An example of the sample spaces considered at three different times for each transverse detonation is shown in frames (A) and (B) in Fig. 5.

Frames (C1)-(C3) and (D1)-(D3) in Fig. 5 summarize our results for the triple point and transverse detonations speeds for the simulation with $p_0 = 13.8$kPa through vector diagrams for the time steps where the shocked gas mixture velocity was measured. In the figures, U_{TD} and U_{TP} refer to the velocities of the transverse detonation and triple point, respectively. $\tilde{U}$ is the mass averaged resultant velocity of the shocked gas mixture that the transverse detonation propagates through, calculated as $\sqrt{\tilde{u_r}^2 + \tilde{u_z}^2}$, where $\tilde{u_r}$ and $\tilde{u_r}$ are the mass averaged r and z velocity components. In frames (C1)-(C3), it is first observed that following the initiation of TD1, the resultant velocity of the shocked mixture not only decays in magnitude as the leading shock weakens but also changes direction as TD1 propagates to the wall. This change in direction is caused by the unconstrained expansion of the leading shock following the decoupling of the shock and reaction zone caused by the diffraction process. The unconstrained expansion then permits TP1 to propagate close to the CJ speed of the quiescent mixture while satisfying the respective vector relations. However, this is not the case for the second transverse detonation, where the expansion of the shocked gases behind the leading shock wave is constrained between TD2 and the tube axis. This is shown in frames (D1)-(D3), with the direction of $\tilde{U}$ relatively fixed. Under the constraints that TP2 must be attached to the transverse detonation and the direction of $\tilde{U}$ is fixed, satisfying the vector relations causes TP2 to be overdriven. In a separate study [7], the authors studied the re-initiation of a quenched detonation wave following its interaction with an obstacle where the triple point attached to the transverse detonation was also overdriven. After further investigation, it was found that the shocked mixture was once again constrained in this case. The results presented here then provide an explanation for the overdriven triple point in this study as well. Ultimately, from the figures, it can be concluded that the second triple point is overdriven simply because the shocked gas mixture is geometrically constrained for this case.

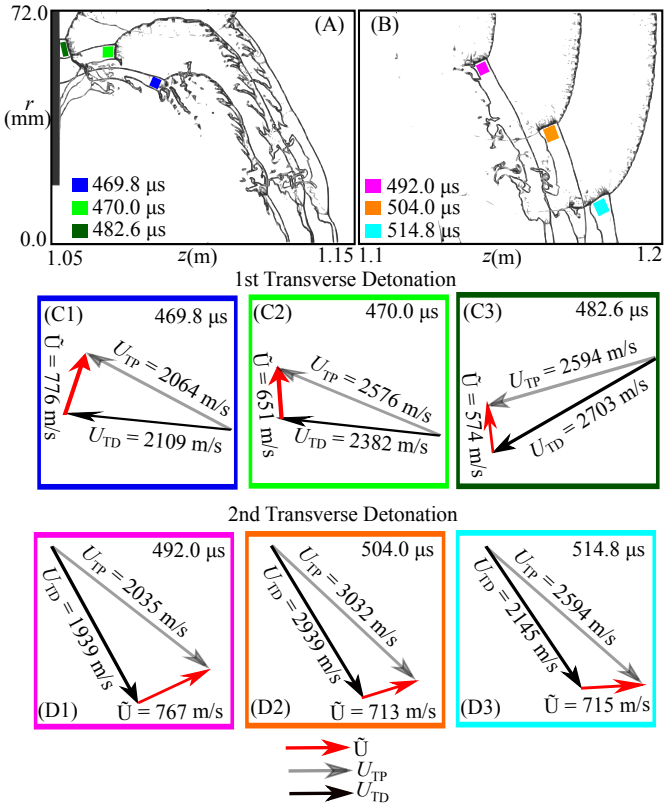

Figure 5: Density gradient composites showing the propagating transverse detonation waves for $p_0 = 13.8$ kPa along with the sample spaces where the shocked gas mixture velocity is extracted from (A and B). Frames (C) and (D) show the magnitude and the direction of the triple point speed (U_{TP}), transverse detonation speed (U_{TD}), and resultant velocity of the shocked mixture for the sample space ($\tilde{U}$) for the first and second transverse detonations respectively.

References

[1] Mohnish Peswani and Brian Maxwell. Detonation wave diffraction in stoi- chiometric C_2H_4/O_2 mixtures using a global four-step combustion model. Physics of Fluids, 34(10):106104, 2022.

[2] M Peswani, C Gerace, and B Maxwell. Combustion properties of a simple and efficient four-step model. Shock Waves, 32(6):517–537, 2022.

[3] E. Schultz, Detonation diffraction through an abrupt area expansion, Ph.D. thesis, California Institute of Technology (2000).

[4] J.H.S. Lee and I.O. Moen. The mechans of transition from deflagration to det- onation in vapor cloud explosions. Progress in Energy and Combustion Sci- ence, 6(4):359–389, 1980.

[5] M. Kuznetsov, M. Liberman, and I. Matsukov. Experimental study of the preheat zone formation and deflagration to detonation transi- tion. Combustion Science and Technology, 182(11-12):1628–1644, 2010.

[6] C. Wang, C. Qian, J. Liu, and M.A. Liberman. Influence of chem- ical kinetics on detonation initiating by temperature gradi- ents in methane/air. Combustion and Flame, 197:400–415, 2018.

[7] G. Floring, M. Peswani, and B. Maxwell. On the role of transverse detonation waves in the re-establishment of attenuated detona- tions in methane–oxygen. Combustion and Flame, 247:112497, 2023.